

---

# Investigation on Crack Repairing Technique to Delay Fracture Initiation of Steel Members Subjected to Low Cycle Fatigue

---

[S. Abeygunasekara](#) , [J.C.P.H Gamage](#) \* , [S Fawzia](#)

Posted Date: 20 September 2023

doi: 10.20944/preprints202309.1367.v1

Keywords: steel members; crack stop hole (CSH); CHS/CFRP hybrid composite; low cycle fatigue; average tensile strength



Preprints.org is a free multidiscipline platform providing preprint service that is dedicated to making early versions of research outputs permanently available and citable. Preprints posted at Preprints.org appear in Web of Science, Crossref, Google Scholar, Scilit, Europe PMC.

Copyright: This is an open access article distributed under the Creative Commons Attribution License which permits unrestricted use, distribution, and reproduction in any medium, provided the original work is properly cited.

Article

# Investigation on Crack Repairing Technique to Delay Fracture Initiation of Steel Members Subjected to Low Cycle Fatigue

S. Abeygunasekara <sup>1</sup>, J.C.P.H Gamage <sup>2,\*</sup> and S. Fawzia <sup>3</sup>

<sup>1</sup> University of Moratuwa 1; abeygunasekarasampath@gmail.com

<sup>2</sup> University of Moratuwa; kgamage@uom.ac.lk

<sup>3</sup> Queensland University of technology

\* Correspondence: kgamage@uom.ac.lk

**Abstract:** The stress concentrations have become common phenomenon of steel elements when arresting a fracture by implementing the crack stop hole (CSH) technique. Embedding the CSH with Carbon Fibre Reinforced Polymer (CFRP) enhance the fatigue life by delaying the fractures while achieving a stiffness recovery due to superior mechanical characteristics of CFRP material. Hence, low cyclic fatigue (LCF) behaviour of 162 strengthened and non-strengthened CSH specimens were examined in this context. These specimens were subjected to a range of 0 to 10,000 fatigue load cycles with the frequency of 5 Hz. At the end of fatigue exposure, the average tensile strength was measured in each case. The average strength reductions in the range between 13% to 25% was noted in steel elements with CSH subjected to fatigue exposure. The application of a CFRP patch on CSH had effectively recovered the strength losses while enhancing the strength in the range between 32% to 45% with respect to the non-strengthened non specimens. The developed numerical model based on cyclic J-integral technique agrees with test results and is capable of predicting characteristics for this novel hybrid technique.

**Keywords:** steel members; crack stop hole (CSH); CSH/CFRP hybrid composite; low cycle fatigue; average tensile strength

## 1. Introduction

Aged structures are vulnerable for fatigue due to material degradation and heavy loads resulted from increased present service demand [1]. Fatigue usually causes in fractures at micro structural level which cannot be observed visually [2]. According to the previous investigations, 90 % of structural failures occur due to fatigue fractures [3]. Also, fatigue cracks in steel elements may accelerate due to stress concentrations. End results of fatigue is unrecoverable failure of structures and loss of lives and properties.

The CSH technique is a proven technique for crack control and it could be considered a quick, simple and a cost effective method. The procedure of the CSH technique is drilling a hole at the end of crack tip, to convert the crack into a notch. The result is the reduction of stress on the cracked structural elements. This technique was successfully utilized in aerospace industries since 1950 [4] and at present steel bridge repairing applications have also introduced this method. However, reduction of stiffness and re-cracking due to continuous service loads could be considered a major drawback of this technique.

A study carried out by Fish et al. have recommended a range of CSH diameter between 50 mm and 100 mm for effective performance [5] while Ishikawa et al. recommended a range of diameter between 6 mm to 25 mm [6]. The practical applications have confirmed a minimum requirement for the hole diameter which is 25 mm [7] the formula developed by Rolfe and Barsom in 1977. Fisher et al in 1980 introduced a co relation to estimate the size of the CSH. This clearly indicates the size of

the CSH is a main debate in this technique and needs some appropriate design guidelines to decide the size of the CSH under fatigue.

CFRP materials have been successfully applied to restore the degraded steel structures since 1980 [8] because of the resistance to corrosion, its light weight and a remarkable fatigue durability [9]. CFRP material has the capacity to reduce the stress intensity factor (SIF) at the crack tip also [9]. Hence, strengthening of the CSH using CFRP material has great potential to arrest the crack and it may enhance the fatigue performance due to delays in cracking by nature. In addition CFRP/steel composite contributes to improve the tensile capacity while extending load bearing capacity which needs to cater for increased demand. This investigation is focused on assessing the performance of CSH/CFRP hybrid system while introducing a design formula for the CSH technique.

## 2. Test program

A total of hundred and sixty-two specimens which were categorized into seven series were tested while the details are listed in Table 1.

**Table 1.** Summary of the test program.

Series	Geometry	Composite action	Conditioning type	Samples
S1	Steel plates with and without a CSH non strengthened	Up to 10,000 cycles with step of 2000 cycle		24
S2	Steel plates with and without a CSH strengthened			24
S3	Steel plates with a CSH with varying diameter of the CSH (control samples)	Non conditioned	strengthened / non-strengthened	24
S4	Steel plates with a CSH with varying diameter of the CSH non-strengthened	10,000 cycles	strengthened /non-strengthened	36
S5	Steel plates with a CSH with change in position non strengthened	10,000 cycles		15
S6	Steel plates with a CSH with change in position		strengthened	10,000 cycles 15
S7	Steel plates with and without a CSH with varying CFRP bond length		strengthened	10,000 cycles 24

The test samples were designed in accordance with ASTM D 790 [10] with the dimensions of 40 mm (width) x 5 mm (thickness) x 280 mm (span) (Figure 1).

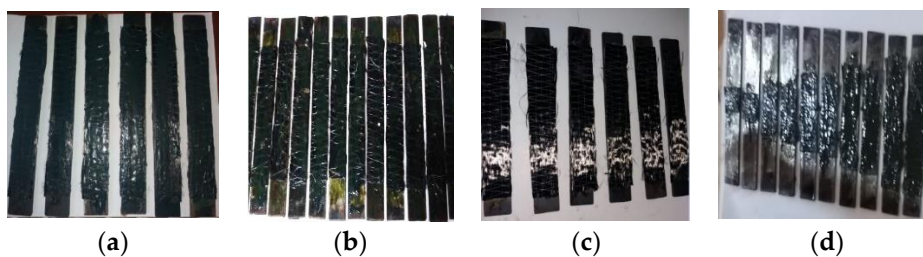


**Figure 1.** prepared specimens of CFRP strengthened plates (a) without a CSH (b) with CSH (c) with changing position of the CSH (d) with different CFRP bond length.

The surfaces to be strengthened were prepared using sand blasting and the wet layup method was followed in the strengthening process. The prepared samples were kept to cure for 7 days before conditioning. A fatigue load was applied with 2 kN amplitude and frequency of 5 Hz within a predefined duration according to standards [11]. After conditioning with pre-determined number of load cycles the sample was removed from the fatigue testing machine and it was fixed to the universal tensile testing machine (UTM) with 100 kN capacity to applied tensile load as shown in Figure 2b. This procedure was repeated and the average value of the tensile load was measured for each

specimen. The strain variation at the CSH of the specimen during exposure of fatigue load was recorded using a data logger.

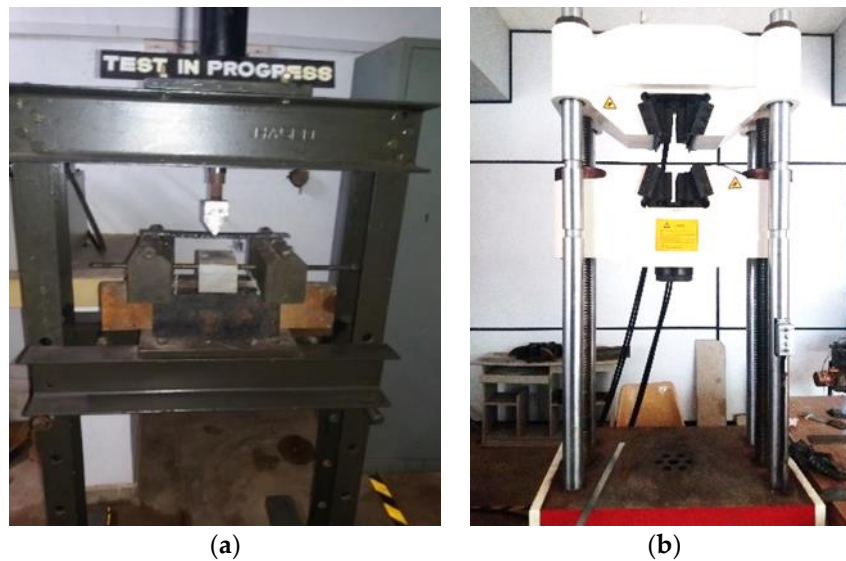


**Figure 2.** Test setup and instrumentation (a) fatigue load setup (b) tensile test setup.

The modulus of elasticity and tensile strength of steel and the CFRP material were determined experimentally by a coupon test. Tensile strength and elastic modulus of the steel were measured according to the ASTM D 3039 standards. In fact, a tensile strength of 583 MPa and an average elastic modulus of 200 GPa were reported. Tensile strength and an average elastic modulus of CFRP material were reported 175 MPa and 1575 MPa respectively. Manufacturers provided data compared with measured material properties in accordance with ASTM D 3039/3039 M [12] are listed in Table 2.

**Table 2.** Measured and manufacturers provided material properties [13–15].

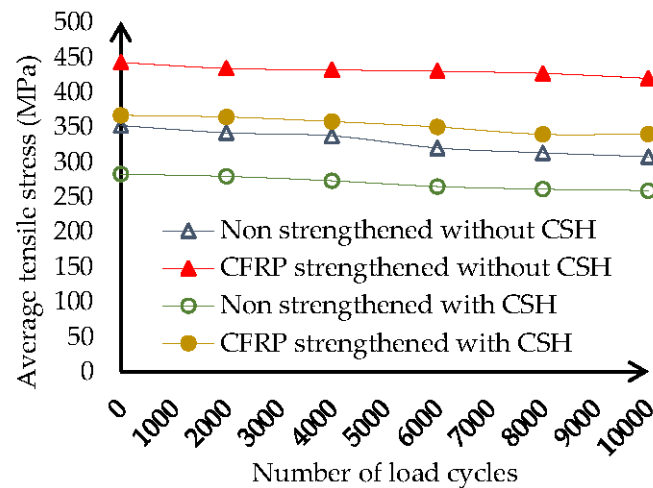
Material property	Measured data			Manufacturers provided data		
	Steel	Epoxy adhesive	CFRP	Steel	Epoxy adhesive	CFRP
Average tensile strength (MPa)	583	25	1575	350	29	550
Average elastic modulus (GPa)	200	0.579	175	200	1.85	240

### 3. Test results

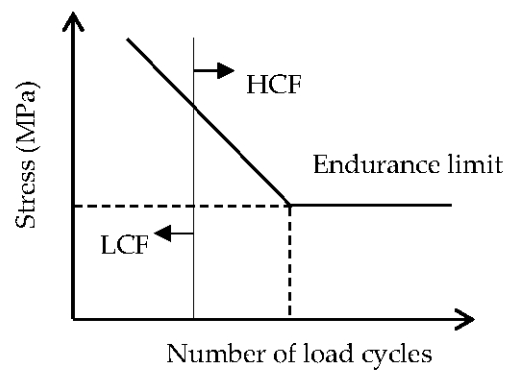
Evaluation of sensitive parameters and their effects on fatigue performance of CSH/CFRP hybrid system is the key objective of this research study. Further analysis of actions, parameters and their effects may yield recommendations on deriving design guidelines for improving the maintenance procedure of steel members exposed to fatigue especially in bridges.

#### 3.1. Effects of conditioning period on LCF performance

Low cycle fatigue (LCF) is typically characterized by the Manson-Coffin relation and investigation results agreed with theoretical behaviour of steel as shown in Figure 3b [16]. A total of forty-eight specimens were tested up to 10,000 load cycles with 2 kN amplitude and 5 Hz frequency ( $S_1$  and  $S_2$ ). Twenty-four samples contained a 16 mm diameter CSH at the centre of mid span which covered with a 200 mm long CFRP sheet symmetrically. The remaining samples ( $S_1$ ) were non strengthened while introducing a CSH of 16 mm diameter at the mid span as a control sample. The average tensile strength variation was determined and compared for each test series at the end of fatigue exposure as shown in Figure 3a.



(a)



(b)

**Figure 3.** Variation of average tensile stress with number of load cycles (a) comparison of test results (b) theoretical curve [17].

When the element is conditioned up to 10,000 cycles (within low cycle fatigue range), the measured average tensile strength slightly decreases with the exposure period, indicating a similar trend irrespective from the sample configuration (Figure 3a). The CFRP/steel hybrid composite CSH indicated a significant fatigue enhancement in the range from 29 % to 32 % when compared with a non-strengthened CSH. This is mainly due to the composite action and ability of dissipating stress concentrations at CSH by the CFRP laminate. In addition, excessive tensile strength and load bearing ability of the CFRP material also contribute for such behaviour. The latter results clearly indicate that the CFRP installation has significantly affected on the strength recuperation of material and had effectively delayed the cracking at the CSH, providing evidence for the merit of suggested hybrid technique in this study to address the critical problem in the bridge maintenance procedure.

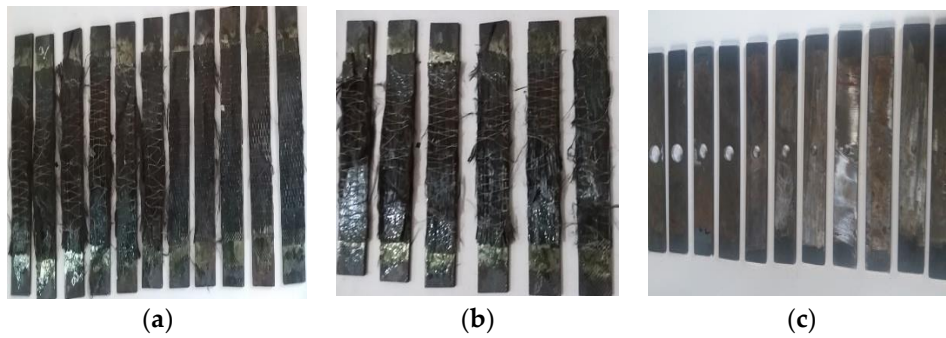


**Figure 4.** Failure mode; strengthened (a) without CSH (b) with CSH (c) non strengthened with CSH.

### 3.2. Effects of CSH diameter on LCF behaviour

A total of sixty samples were tested. Twenty-four of them were not exposure to fatigue (non-conditioned) and considered as a control samples (series-S<sub>3</sub>) and the remaining were conditioned up to 10,000 load cycles with 2 kN amplitude and 5 Hz frequency (series-S<sub>4</sub>). Both strengthened and non-strengthened samples, the ratio between diameter of CSH and width of member ( $d/b$ ) varied from 0.1 to 0.6 in a 0.1 step by positioning the CSH at the centre of mid span. A 200 mm long unidirectional normal modulus CFRP fabric was used to purpose of strength. At the end of the fatigue exposure, the test specimen was fixed with universal tensile apparatus to measured, the tensile load to determined and compare average stress as shown in Figure 5.

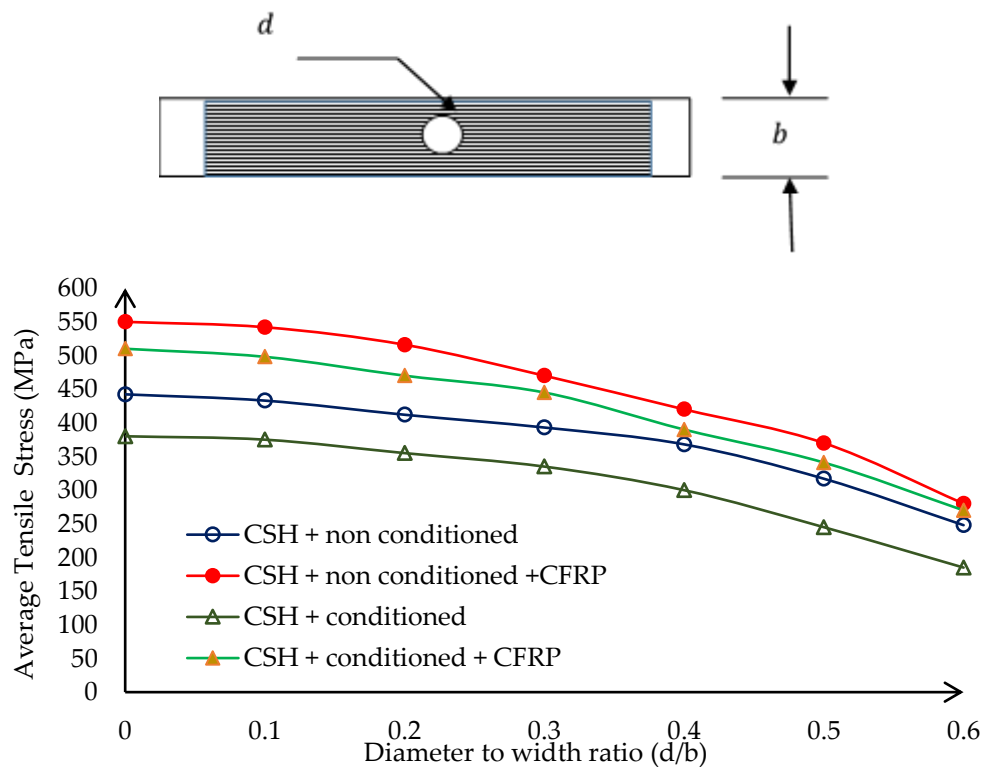


**Figure 5.** Strength losses due to fatigue and strength gains by CFRP.

On average 14% strength loss was noted in the specimen due to fatigue effects even without the CSH. This is mainly due to the material degradation by repetitive loading and unloading action (fatigue). On average 13% to 25% strength loss was noted when the  $d/b$  ratio varies from 0.1 to 0.6 at the end of fatigue exposure in the specimens with the CSH. In general, the CSH causes for reducing the stiffness due to removal of materials. On the other hand, change in microstructures of material near the hole due to fatigue effects. The change in average tensile capacity of the material is governed by the plastic flow effects, imperfections in the crystal lattice of a material, forward and backward motions of dislocations and plastic deformation along the slip planes of metallic crystals. All these

factors are critically affected on a significant strength loss during fatigue exposure on CSH. However, the average tensile strength was enhanced by 24% in the CFRP strengthened CSH system at the end of fatigue exposure. This clearly indicates the ability of recovering the strength loss by CFRP with improved fatigue performance. The suggested system in this study, on average 32% to 45% strength gain was noted when  $d/b$  ratio varies from 0.1 to 0.6 at the end of predetermined fatigue exposure. Therefore, the proposed CSH/CFRP hybrid repairing technique has a potential to enhance the stiffness of member as well as the restoration of fatigue bearing capacity of the material. Failure modes observed during tensile testing of these series are shown in Figure 6.

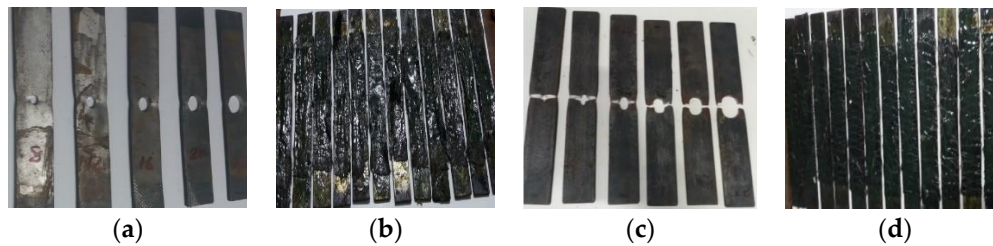


**Figure 6.** Failure mode of CSH; non conditioned (a) non-strengthened (b) strengthened, and conditioned (c) non-strengthened (d) strengthened samples.

Variation of strain near the crack stop hole was monitored during fatigue load application. Conventional strain gauges attached to the steel surface, 5 mm away from the periphery of CSH were used as shown in Figure 7.

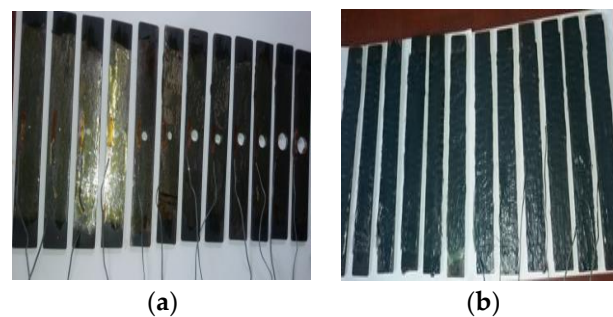


**Figure 7.** Strain gauges attached to the (a) non strengthened (b) CFRP strengthened CSH specimens.

The strain near the CSH at the end of each pre-determined load cycles is plotted in Figure 8.

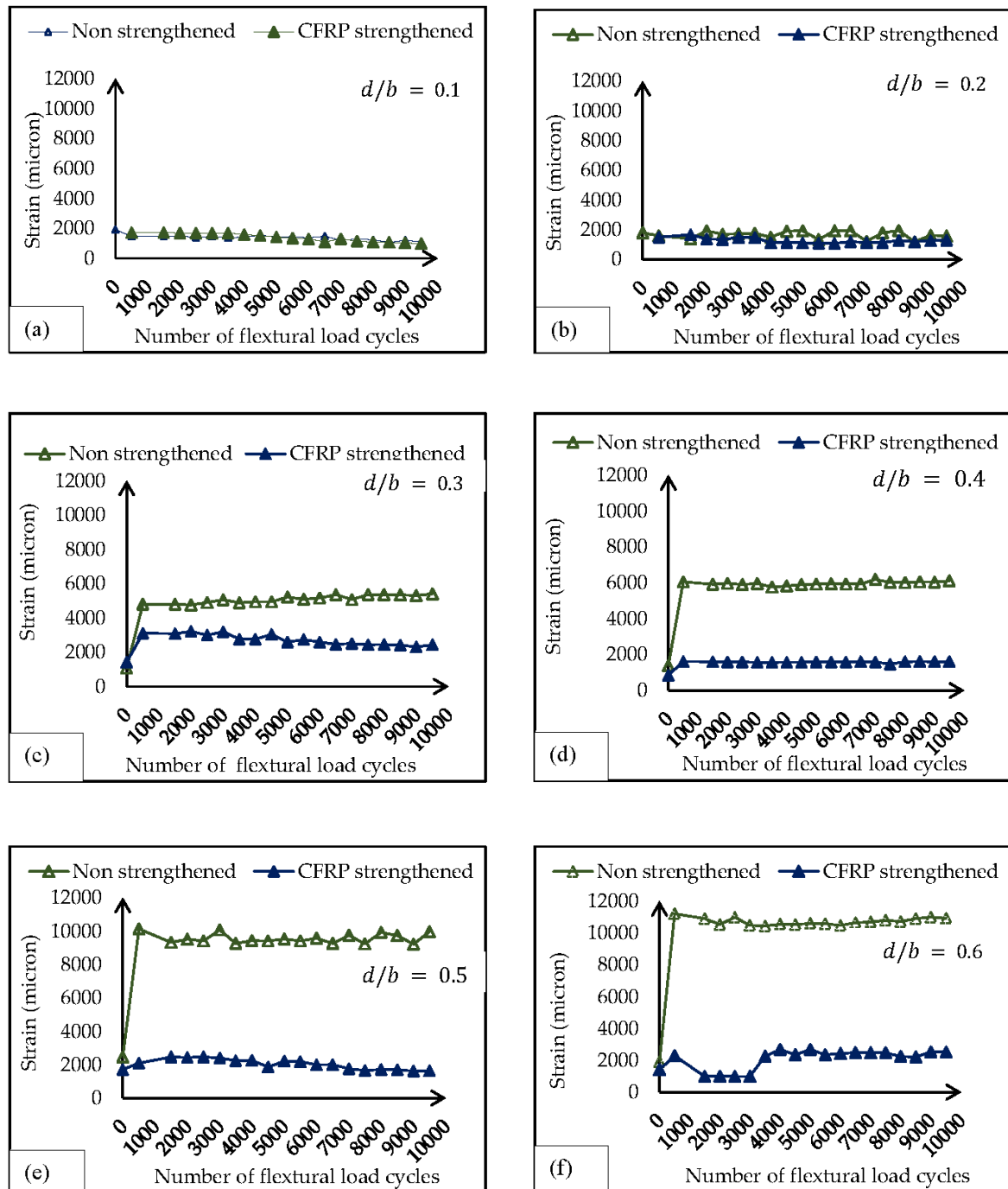


**Figure 8.** Strain variations during conditioning when  $d/b$  is ; (a) 0.1 (b) 0.2 (c) 0.3 (d) 0.4 (e) 0.5 (f) 0.6.

According to Figure 8a,b, no significant deviation was noted in both strengthened and non-strengthened samples. The contribution of CFRP material is negligible and the steel substrate could withstand the effects of fatigue. When  $d/b$  ratio increases from 0.3 to 0.6, the strain variation on the steel substrate of samples with CFRP indicated a significant strain reduction than the non-strengthened CSH as shown in Figure 8c to Figure 8f. This is due to the effective load sharing ability of attached CFRP layer. The results in strain control is contribute to further delaying crack propagation nature of the CSH. Hence, measured strain variation indicates the effectiveness of proposed hybrid repairing technique for steel members exposed to fatigue over the traditional CSH technique.

### 3.3. Effects of the location of CSH on LCF behaviour

A total of thirty-six steel specimens with change in position of the CSH were conditioned up to 10,000 load cycles with 2 kN amplitude and 5 Hz frequency (series -  $S_5$  and  $S_6$ ). Eighteen of them were reinforced with 200 mm long CFRP layer. The remaining samples were non-strengthened and taken in to consideration as controlled specimens. In these two test series, the distance from loading point to CSH was considered as the main variable and a CSH of 16 mm diameter was placed at the pre-determined locations of the member, distance to CSH from mid span varies 20 mm to 100 mm in 20 mm steps. At the end of fatigue loading, the average tensile strength of samples was determined using universal tensile testing apparatus and results is plotted in Figure 9.

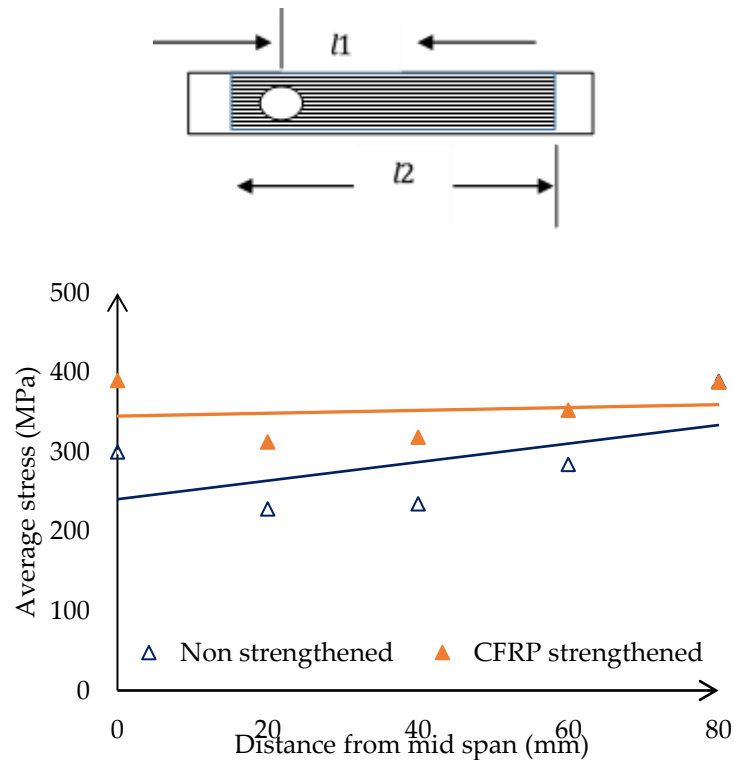
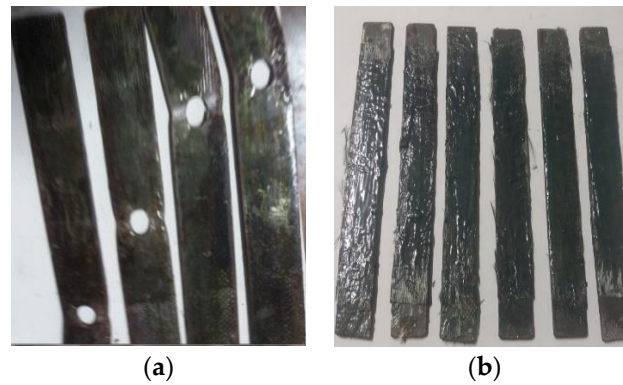


Figure 9. Comparison of average strength variation with CSH position.

The main purpose of this test series was to compare the retained tensile strength after fatigue load exposure to quantify the effectiveness of CFRP on the distance to CSH from mid span. A trend of average retained tensile strength variation deviation with respect to the ratio between diameter to offset distance of CSH was noted from both strengthened and non-strengthened samples. When the offset distance increases reference to the loading point (midpoint of the specimen), the stress concentrations near CSH reduces. The graphs also provide convincing evidence on such behaviour. CFRP layer supports to reduce the stress concentration while enhancing the tensile strength of the specimen. As a result, the CSH/CFRP hybrid system showed a significant strength gain compared to similar non-strengthened specimens which restored the strength loss due to the opening of the CSH. This clearly indicates the extending the fatigue performance of steel members when applying the suggested hybrid repairing technique in this study, irrespective from the location of CSH with guaranteed performance than the conventional CSH technique. Failure mode was observed as delamination of the CFRP layer (Figure 10b).



**Figure 10.** Failure mechanisms of (a) non-strengthened (b) strengthened samples.

Strain gauges were fixed near the specimens as shown in Figure 11. The average strain variation during fatigue was measured at the end of each pre-determined load cycles as shown in Figure 12, based on the distance to CSH ( $x$ ) from the mid-point. When the CSH is near the mid span, it subjects to heavy stresses which dissipate by the CFRP sheet. As a result there is a comparatively lower strain in steel substrate of hybrid arrangement (Figure 12a) when compared with the conventional CSH arrangement. When the position of the CSH moves from the centre to the support, the fatigue stresses also reduces. Hence, similar strain variation was observed in both strengthened and non-strengthened samples. This clearly indicates that the proposed CSH/CFRP hybrid arrangement could successfully accommodate the strain near the CSH.

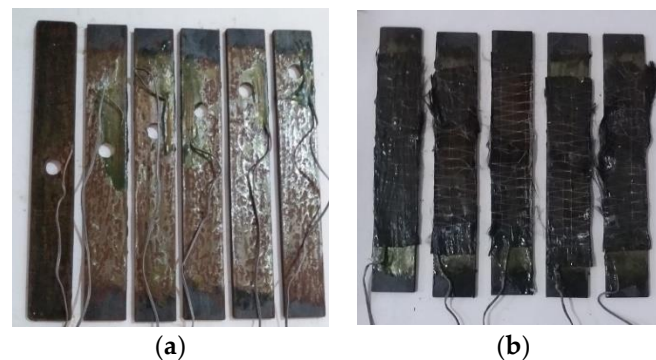


**Figure 11.** Strain gauges fixed to the (a) non strengthened (b) strengthened specimens.

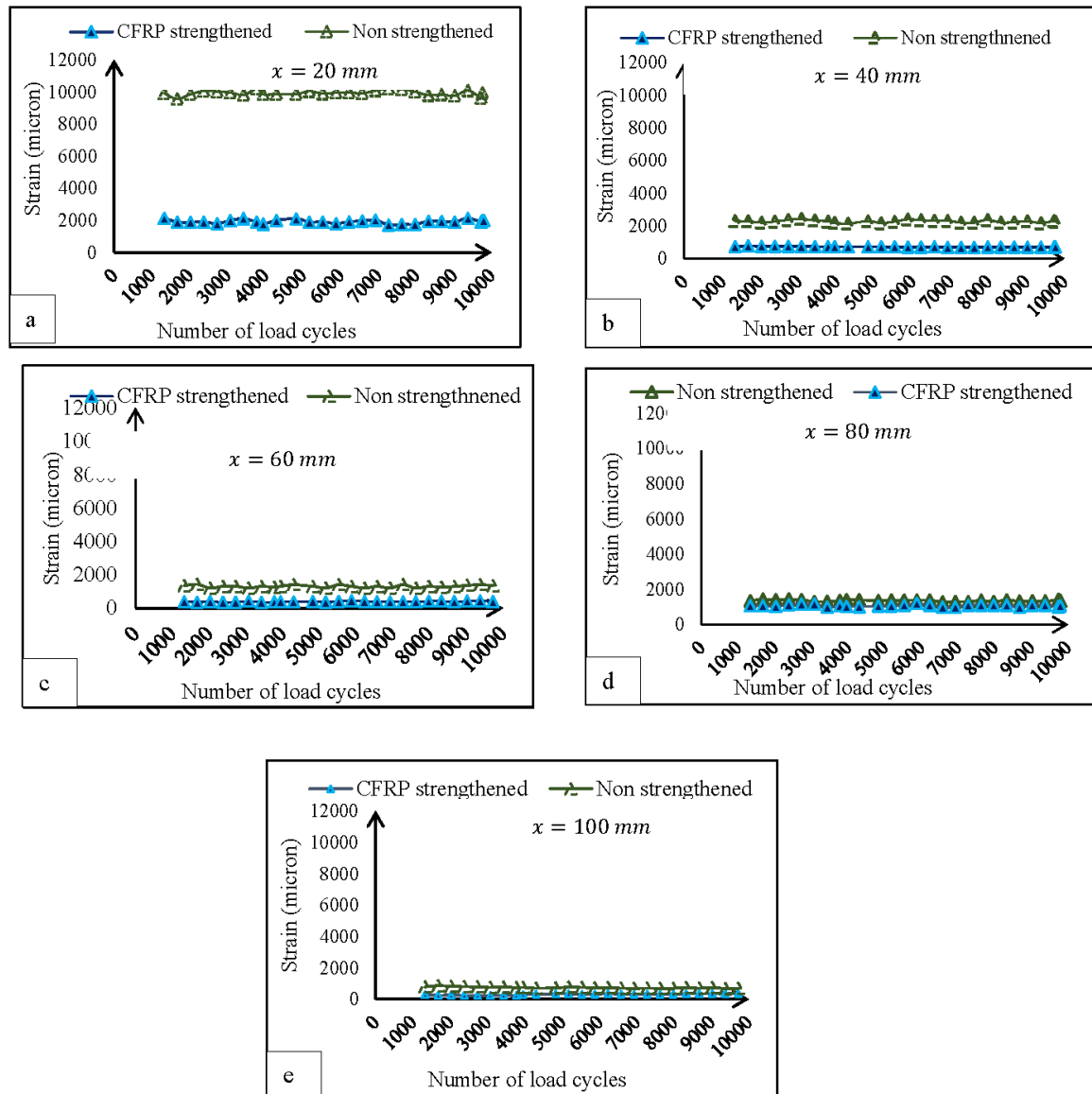


**Figure 12.** Comparison of strain variations with distance to the CSH from mid-point for non-strengthened and CFRP strengthened CSH when  $x$  is ; (a) 20 mm (b) 40 mm (c) 60 mm (d) 80 mm (e) 100 mm

### 3.4. Effects of CFRP bond length on LCF behaviour

A total of twenty-four steel specimens with and without a CSH were conditioned up to 10,000 fatigue cycles of 2 kN constant amplitude and 5 Hz frequency (series – S<sub>7</sub>). A 16 mm diameter CSH was placed at the mid-span of twelve specimens and remaining samples were prepared without a CSH as a control sample. The length of the CFRP sheet was considered as the principle variable and varied from 20 mm to 120 mm in 20 mm step, was attached symmetrically, covering the CSH (Figure 13). CFRP strengthened steel plates without a CSH showed an increasing linear trend between retained tensile strength at the end of fatigue exposure. This is mainly due to the direct contribution of CFRP layer to enhance the tensile strength of specimen. A linear relationship was noted between retained tensile strength and CFRP bond length of samples with a CSH, subjected to fatigue exposure. Furthermore, the CFRP layer helped to strengthen the recovery while enhancing the tensile strength of member. Interestingly, CFRP materials possess excellent fatigue strength. These reasons may cause for the increasing trend between retained tensile strength with respect to CFRP bond length.

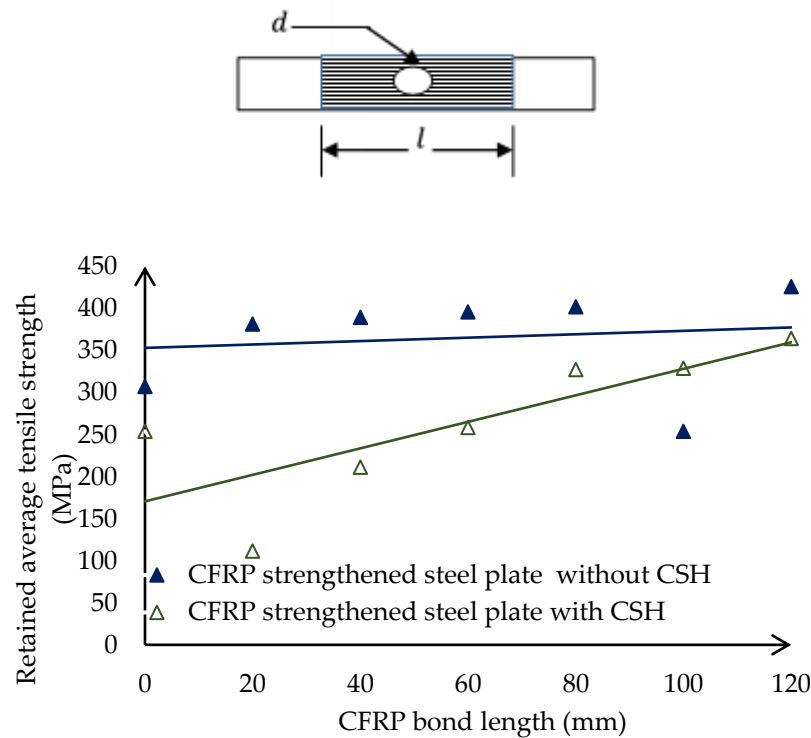


**Figure 13.** Strength variation with the bond length.

The CFRP material is capable of decreasing stress as well as enhancing the fatigue load bearing capacity of the specimen. However, steel failure does not occur during the fatigue load. When performing the tensile test on the conditioned specimen, it starts to propagate cracks in a perpendicular direction of the CSH as shown in Figure 14a. The CFRP layer experienced de-laminate as shown in Figure 14b.

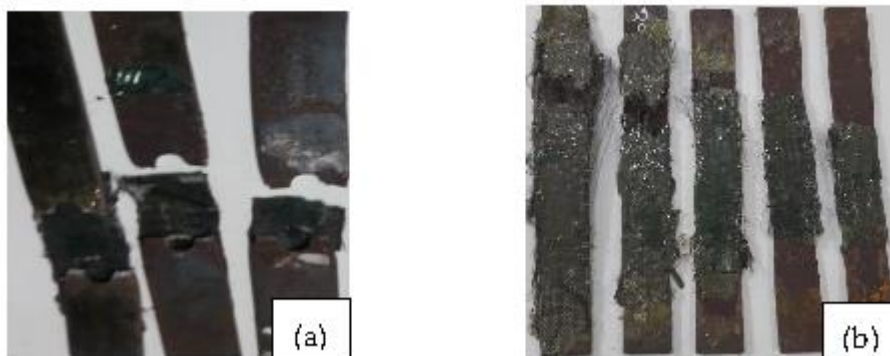


**Figure 14.** Failure mode of CFRP strengthened specimen with bond length (a) with CSH (b) without CSH.

#### 4. Finite element modelling(FEM)

A numerical model was developed to simulate the performance of CSH/CFRP hybrid technique using a commercially available finite element software [18]. The geometrical configuration, boundary conditions, material properties and attributes as the same as in test program was used in the modelling process. A general contact standard type was utilized with mechanical friction to simulate the interfaces between two supportive rollers and the bottom surface of the plate, and the loading nose on the mid plane of the steel plate as shown in Figure 15 [19]. Each specimen model was loaded with the LCF mode using a direct cyclic option [19]. When the size of the mesh is very small it results in generating a singularity point. Stress at the singularity points are theoretically considered as

infinity. Therefore, considering all of above factors, an FEM result of 2 mm mesh size was selected as an appropriate size in this analysis.

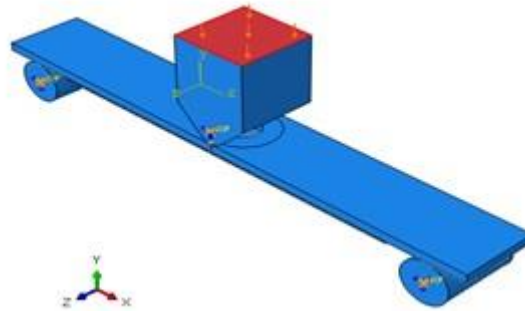


**Figure 15.** The assembly model of the specimen.

The magnitude of pressure applied on top of the loading nose was selected as  $1.25 \text{ N/mm}^2$  (2 kN) and the frequency of loads was fixed as 5 Hz. When considering the boundary conditions, two supportive cylinders were fixed to avoid both rotation and translation. Loading rate was kept as a constant at a fixed rate of 0.2 mm/min throughout the analysis. Three dimensional 8 node solid brick elements with reduced integration (C3D8R) were used to mesh the steel plate, supportive rollers and loading nose components [19]. The Hashin damage option was used to model the CFRP fabric [17].

Basically two tests series were considered in this background as diameter to width ratio and position of the CSH variation. Diameter to width ratio was changed from 0.1 to 0.6 and remaining available parameters were kept as a constant during the analysis. In case of location of CSH effect, offset distance vary from 0 to 80 mm in 20 mm steps with respect to mid-point and all remaining parameters were kept as a constant during the analysis. The model was identical with configurations of the laboratory test setup. Results of laboratory test and FEM results were compared to validate the developed model. Contours of stress variation with diameter for non-strengthened and CSH/CFRP hybrid system shown in Figure 16a and Figure 16b, respectively.

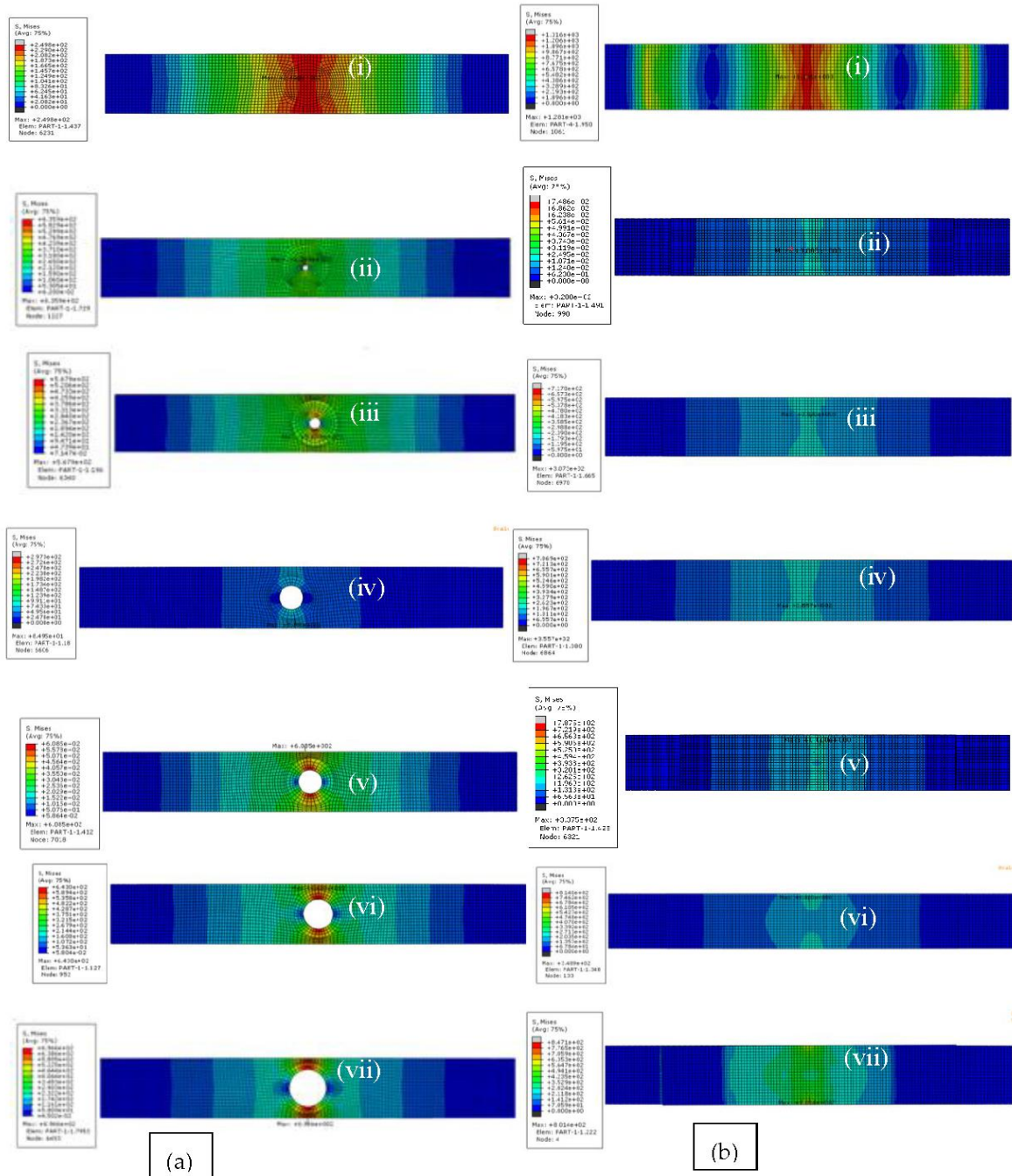


**Figure 16.** Contours of stress variation with diameter to width ratio for (a) non-strengthened (b) CSH/CFRP hybrid (i) 0 (ii) 0.1 (iii) 0.2 (iv) 0.3 (v) 0.4 (vi) 0.5 (vii) 0.6.

The effect of diameter to width ratio of CSH was taken into consideration as a primary variable in this analysis. The predicted results belong to non-strengthened and CSH/CFRP hybrid (after fatigue exposure) were compared with relevant laboratory test results as in Figure 17.

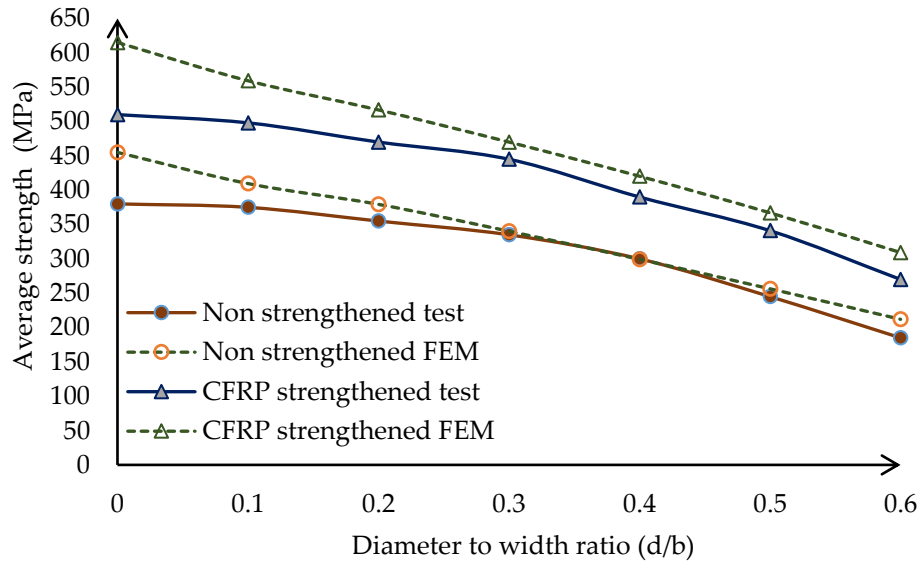


**Figure 17.** Comparison between experimental and predicted results - series; (a) S<sub>3</sub> and S<sub>4</sub> (b) S<sub>5</sub> and S<sub>6</sub>.

Contours of stress variation with offset distance for non-strengthened and CSH/CFRP hybrid system shown in Figure 18a and Figure 18b, respectively.

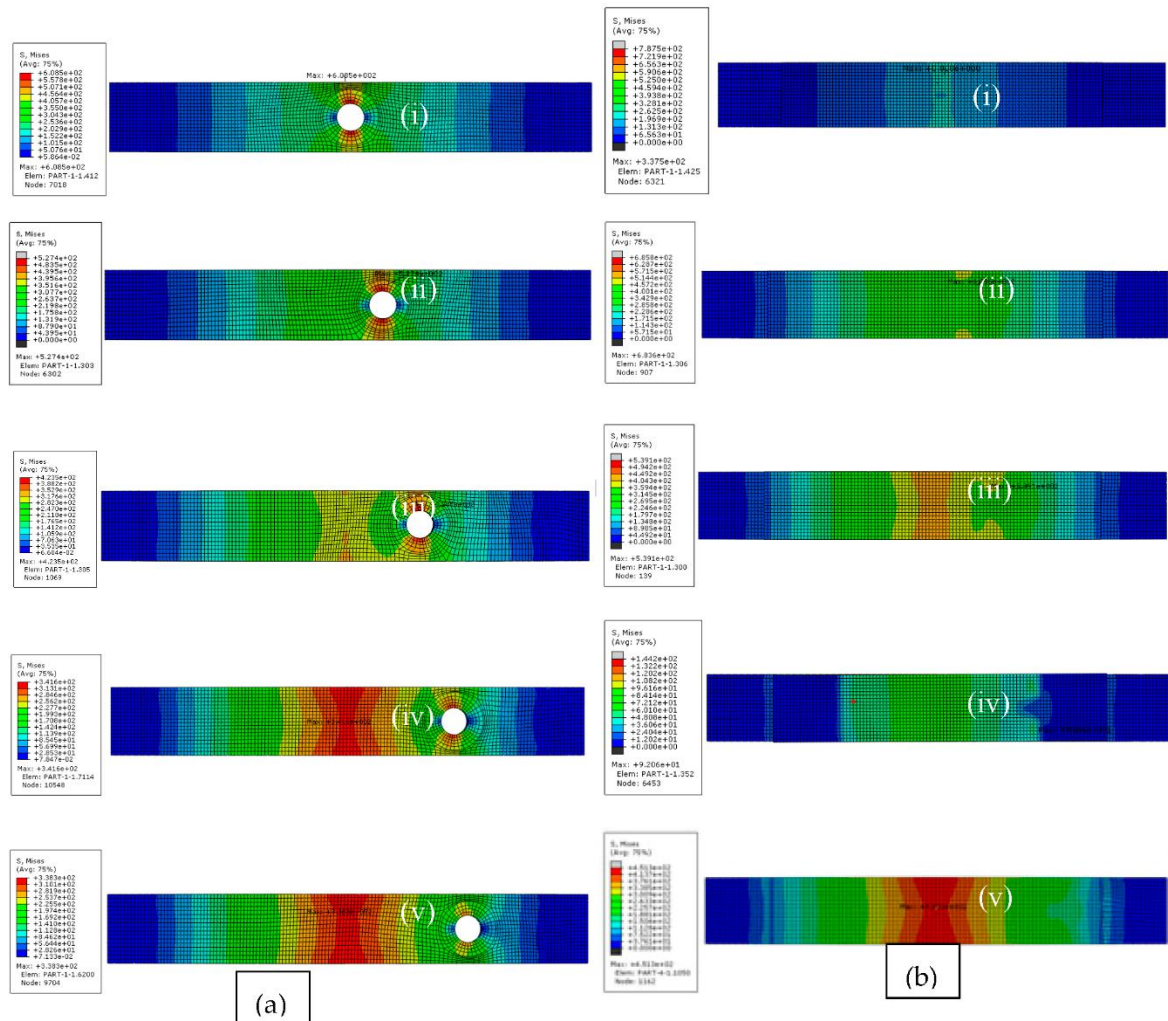


**Figure 18.** Contours of stress variation with distance from mid-point for (a) non-strengthened (b) CSH/CFRP hybrid system (i) zero (ii) 20 mm (iii) 40 mm (iv) 60 mm (v) 80 mm.

The effect of offset distance of the CSH was taken into consideration as a primary variable and it varied from 0 to 80 in 20 mm steps. The predicted results belonging to non-strengthened and CFRP strengthened (after fatigue exposure) were compared with relevant experimental results as in Figure 19.

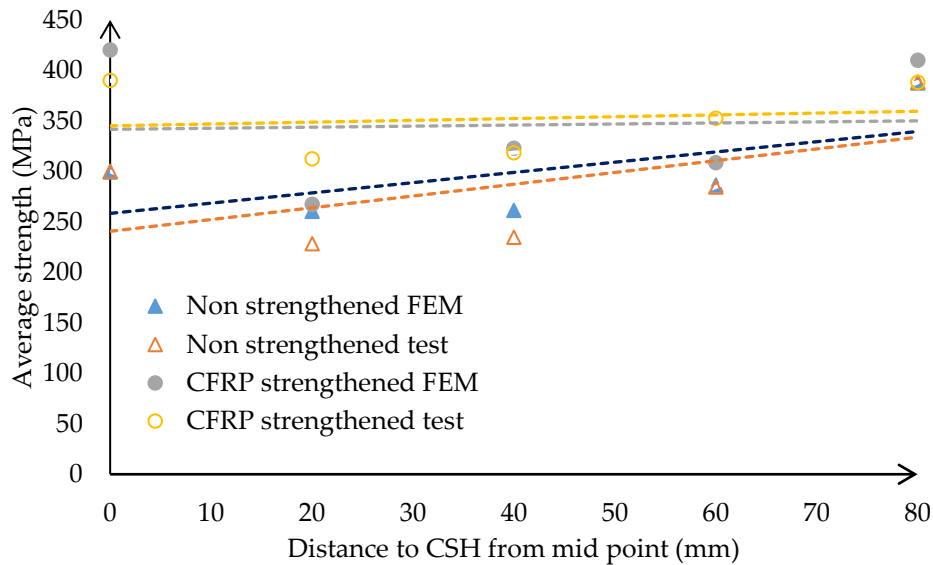


**Figure 19.** Comparison between experimental and predicted results - series; (a)  $S_3$  and  $S_4$  (b)  $S_5$  and  $S_6$ .

The model predicted results of conditioned CSH samples indicates on average 5 % and 7 % difference with tested results for non-strengthened and CFRP strengthened samples, respectively in Figure 19. When the distance to CSH from the mid-point varies, the average deviations between predicted and tested results of non-strengthened and CFRP strengthened samples are 7 % and 8 %, respectively (Figure 19). This clearly indicates the accuracy of developed models that could be used to further simulate the behaviour of suggested CSH/CFRP hybrid system.

#### 4.1. Parametric study

A numerical model was utilized to investigate parametric influences on the CSH. This study member thickness, amplitude of loads, stress ratio, crack length and fiber direction angle were selected as a critically influencing parameters in the range considered. According to the experimental program the diameter of the CSH, the position of the CSH and bond length effects were experimentally investigated and test results have confirmed significant effects for those parameters. Experimental and parametric study results were utilized to introduce design guidelines to estimate the appropriate size of the CSH and guidelines are shown in Table 3.

**Table 3.** Fatigue related design guidelines for CSH.

Category	Parameter	Range of Operation
Geometry	Diameter to width ratio ( $d/b$ )	$\frac{d}{b} \leq 0.2$

	Thickness to diameter ratio (t/b)	$\frac{t}{d} \leq 0.5$
	Diameter to crack length ratio (d/l)	$\frac{d}{l} \geq 0.4$
	Diameter to offset distance ratio (d/x)	$\frac{d}{x} \leq 0.2$
Load	Ratio of diameter to stress ratio (d/R)	$\frac{d}{R} \geq 80$
	Diameter to frequency ratio (d/f)	$\frac{d}{f} \geq 3$
	Diameter to load ratio (d/F)	$\frac{d}{F} \geq 3$
CFRP	Diameter to bond length ratio (d/L)	$\frac{d}{L} \leq 0.1$

## 5. Conclusions and recommendations

The detailed experimental and numerical simulations conducted on the developed novel hybrid technique to control cracks of steel elements in civil engineering infrastructures yield following conclusions:

1) Diameter of the CSH was a one main argument in available literature and there are no clear guidelines to decide if it considers the effects of critical parameters. In this study, the effects of several parameters were experimentally and numerically estimated while the critical effects on final results were based on geometry with loading and CFRP material characteristics. Using those results this study has introduced design guide lines to decide the appropriate size of the CSH for crack control to delay fracture failures on steel structures due to fatigue.

2) Average strength reductions in the range between 13% to 25% were measured subjected to low cycle fatigue exposure. This is due to the CSH effectively recovering the strength losses while enhancing the strength in the range between 32% to 45% with respect to the non-strengthened non conditioned material features.

3) A novel CSH/CFRP hybrid system in this study could be utilized successfully to eliminate the main drawbacks related to the CSH technique. This method exhibits a significant capacity enhancement for crack controls and is strongly recommended to improve the service life of steel infrastructures under fatigue load.

4) The proposed numerical model in this study validates well as it uses the measured data during the experiment. Hence, this developed numerical model can be effectively utilized to estimate effects of unknown parameter of the CSH under fatigue response.

5) A numerical model could be utilized to investigate invisible characteristics by the experiment and the developed numerical model was prognosticating the range of stress intensity variation, stress variation along crack direction, prediction of the direction of maximum tangential stress which was compared for CSH/CFRP hybrid system with respect to a non-strengthened CSH. Numerical results have confirmed the potential of CFRP utilized ones that enhances the fatigue life of structure.

### 5.1. Future work

Fatigue is governed by the micro structure of a material due to external or internal stress. Therefore, there should be a microscopic analysis regarding grain arrangement, dislocation, and information regarding missing atoms of the material with critical parameters. The finite element model does not have a facility to model the effects of environmental factors on bond performance. This could be considered as a significant gap of FEM techniques. Furthermore, evaluating the long term bond performance relating investigations of the CSH/CFRP hybrid system to confirm durability of this technique could also be carried out in the future.

**Acknowledgements:** The authors gratefully acknowledge the support of the staff of the structural testing laboratory, as well as the staff in computer laboratory. Department of Civil Engineering, University of Moratuwa, Sri Lanka for their valuable support.

**Declaration of competing interest:** The authors declare that they have no known competing or financial interests or personal relationships that could have appeared to influence the work reported in this paper.

### References

1. Vatandoost, F. (2010). *Fatigue behaviour of steel girders strengthened with prestressed CFRP strips* (Master's thesis, University of Waterloo).
2. Božić, Ž., Mlikota, M., & Schmauder, S. (2011). Application of the  $\Delta K$ ,  $\Delta J$  and  $\Delta CTOD$  parameters in fatigue crack growth modelling. *Tehnički vjesnik*, 18(3), 459-466.
3. Committee on Fatigue and Fracture Reliability of the Committee on Structural Safety and Reliability of the Structural Division, American Society of Civil Engineers. (1982). Fatigue reliability: Development of criteria for design. *Journal of the Structural Division*, 108(1), 71-88.
4. Arcovio, S. D. (2013). Fatigue performance of a hybrid CFRP/steel splice detail for modular bridge expansion joints. Queen's University (Canada).
5. Fish, P., Schroeder, C., Connor, R. J., & Sauser, P. (2015). Fatigue and Fracture Library for the Inspection, Evaluation, and Repair of Vehicular Steel Bridges.
6. Ishikawa, T., Matsumoto, R., Hattori, A., KAWANO, H., & YAMADA, K. (2013). Reduction of stress concentration at edge of stop hole by closing crack surface. *Journal of the Society of Materials Science, Japan*, 62(1), 33-38.
7. Dexter, R. J., & Ocel, J. M. (2013). Manual for repair and retrofit of fatigue cracks in steel bridges (No. FHWA-IF-13-020). United States. Federal Highway Administration.
8. Sveinsdóttir, S. L. (2012). Experimental research on strengthening of concrete beams by the use of epoxy adhesive and cement-based bonding material (Doctoral dissertation).
9. Ghafoori, E., & Motavalli, M. (2016). A retrofit theory to prevent fatigue crack initiation in aging riveted bridges using carbon fiber-reinforced polymer materials. *Polymers*, 8(8), 308.
10. "International, A. S. T. M. (2007). Standard test methods for flexural properties of unreinforced and reinforced plastics and electrical insulating materials. ASTM D790-07.
11. "ASTM D7774-12, Standard Test Method for Flexural Fatigue Properties of Plastics," D20.10.24, Ed. West Conshohocken, PA ASTM Int., 2013.
12. Chandrathilaka, E. R. K., Gamage, J. C. P. H., & Fawzia, S. (2019). Mechanical characterization of CFRP/steel bond cured and tested at elevated temperature. *Composite Structures*, 207, 471-477.
13. [online] Available at: <[https://www.researchgate.net/figure/Mechanical-properties-of-the-CFRP-sheet-MBrace-CF-130-based-on-the-fibre-properties\\_tbl2\\_43511771](https://www.researchgate.net/figure/Mechanical-properties-of-the-CFRP-sheet-MBrace-CF-130-based-on-the-fibre-properties_tbl2_43511771)> [Accessed 27 September 2022].
14. [online] Available at: <<https://5.imimg.com/data5/SELLER/Doc/2021/7/FV/NX/RH/130557397/araldite-ft->

- 420-ab-en.pdf> [Accessed 27 September 2022].
15. Matweb.com. 2022. MatWeb - The Online Materials Information Resource. [online] Available at: <<https://www.matweb.com/search/datasheet.aspx?bassnum=MS0001&ckck=1>> [Accessed 27 September 2022].
  16. Coffin Jr, L. F. (1954). A study of the effects of cyclic thermal stresses on a ductile metal. *Transactions of the American Society of Mechanical engineers*, 76(6), 931-949.
  17. Silva, M. A. L., Dedigamuwa, K. V., & Gamage, J. C. P. H. (2021). Performance of severely damaged reinforced concrete flat slab-column connections strengthened with Carbon Fiber Reinforced Polymer. *Composite Structures*, 255, 112963.
  18. Systèmes, D. (2013). ABAQUS 6.13 analysis user's guide. Dassault Systèmes.
  19. Kabir, M. H., Fawzia, S., Chan, T. H. T., Gamage, J. C., & Bai, J. B. (2016). Experimental and numerical investigation of the behaviour of CFRP strengthened CHS beams subjected to bending. *Engineering Structures*, 113, 160-173.

**Disclaimer/Publisher's Note:** The statements, opinions and data contained in all publications are solely those of the individual author(s) and contributor(s) and not of MDPI and/or the editor(s). MDPI and/or the editor(s) disclaim responsibility for any injury to people or property resulting from any ideas, methods, instructions or products referred to in the content.